A STUDY OF CUTTING EDGE GEOMETRY CHANGE AND SURFACE ROUGHNESS IN DRILLING OF CARBON FIBER REINFORCED PLASTICS (CFRP) USING UNCOATED AND COATED TOOLS

Mohammad Sayem Bin Abdullah[1], Dinh Nguyen[2], Dave Kim[3]

[1]Department of Mechanical Engineering, University of Washington, Seattle, WA 98105.

[2]Department of Mechanical Engineering, Michigan State University, East Lansing, MI 48824.

[3]School of Engineering and Computer Science, Washington State University, Vancouver, WA 98686.

ABSTRACT

Cutting edge geometry is a great research concern in machining. This paper investigates the effects of tool wear on cutting edge geometry change, consequent effect of cutting edge geometry on inner hole surface roughness in drilling of CFRP. A drilling experiment has been conducted on CFRP using one uncoated carbide drill bit and two coated carbide tools, namely BAM (BAlMg4) and (AlCrSi/Ti)N. Sharp, honed, chamfered, chamfered induced honed cutting edge has been found in CFRP drilling in this investigation. The sharp tool edge transforms into honed and chamfered due to tool wear in subsequent drilling. The coatings delay the edge geometry changes. The surface roughness of the holes has been measured across the half hole at three consecutive holes in every 40 holes interval holes up to 120 holes. Upon clustering the cutting edges of the three drill bits, the paper investigates the tool edge geometry relation with surface roughness parameters (Ra, Rq, Rz, Rt, Rp, Rv) for each drill bits. The results show that cutting edge geometry has a strong influence on the surface roughness in the drilling of CFRP. Chamfered edge created the largest roughness, while the roughness decreased when the chamfered edges turn to chamfered and honed.

Keywords: Carbon Fiber Reinforced Plastics (CFRP), Tungsten carbide (WC), BAM, (AlCrSi/Ti)N, Drilling, Cutting edge geometry
Corresponding author: [*]Mohammad Sayem Bin Abdullah, Email: sayemab@uw.edu
[*] A previous graduate student at Washington State University, Vancouver, WA

1. INTRODUCTION

The application of Carbon fiber reinforced plastics (CFRP) is increasing in many industries, including aerospace and automobile due to its high specific strength, high specific stiffness, high fatigue resistance, low density, low thermal expansion, corrosion resistance, and excellent damping properties [[1–7]. As polymer matrix is used as the matrix material with carbon fiber as reinforcement, CFRP cannot be welded like metal and other counterparts [8]. Hence, mechanical fastening is the most widespread means of assembling CFRP to other structures due to its

Copyright 2020. Used by the Society of the Advancement of Material and Process Engineering with permission.

simplicity, lower-risk involved in joining, and ease of repair [8,9]. Conventional drilling is the most widely used process for making holes in CFRP plates and many industries, i.e., aerospace, require strict tolerance on CFRP holes [10,11]. One of the important tolerance is posed on surface roughness as the very rougher surface may affect strength, load-bearing capacity, and fatigue life of CFRP[12,13]. The highest acceptable Ra value of in drilling and edge trimming of CFRP-metal stack and CFRP are 3.2 μm and 4.8 μm [11,14]. Defective holes generated by drilling are reported because of the removal of 60% of the composite parts [9,13]. The surface roughness is believed to be the result of severe tool wear as the tool becomes dull and loses its sharpness. Such a dull tool eventually pushes the fiber instead of cutting or fracturing, thereby creates a rougher surface. The cutting edge of cutting tool interacts with the workpiece; thus, the geometry changes due to tool wear and continuous interactions. The tool edge geometry, also known as microgeometry of the cutting tool, may have a relationship with surface roughness. Zhao et al. and Denkena et al. reported that various types of micro-geometry in the machining of metal like steel and metal matrix composite[13–18]. They categorized the cutting edge in sharp, honed, chamfered, chamfered and honed. An illustration of their finding has been shown in a later section of this paper, in Figure 3. Zhao et al. studied the relation of microgeometry on surface roughness in machining metal [21,22]. They reported that the cutting edge strength becomes stronger and creates a rougher surface. Samuel Raj and L. Karunamoorthy the effects of microgeometry on surface roughness along with other parameters, where they reported the proportion relation of peak flattening and cutting edge flattening with surface roughness [23].

In this paper, the relationship of surface roughness of Carbon Fiber Reinforced Plastics (CFRP) hole and cutting edge geometry obtained due to tool wear is investigated in a drilling experiment. This drilling experiment was conducted to compare the effectiveness of the ceramic coated (BAM coating, (AlCrSi/Ti)N coating, and the uncoated tool and the results are published in our previous publication [4]. However, the goal of this paper is to investigate any potential relation of tool micro geometry (cutting edge geometry) and surface roughness. This paper provides a hint to the future direction of evaluating cutting edge geometry and roughness relationship in composite machining.

2. EXPERIMENTATION

2.1 Experimental Set-Up

The drilling experiment was carried out in a three-axis vertical CNC milling machine (Mini-Mill, HAAS, USA). A quasi-isotropic CFRP plate of $[(0/45/90/-45)4/90/02/0\bar{]}s$ was drilled using three different types of coated and uncoated tool. The CFRP panel provided by the Boeing Company. The thickness of the CFRP plate was 7.62 mm, with an average ply thickness of 0.1885 mm and an average fiber diameter of 5 microns. The tools used were; uncoated (Grain size = 0.7 μm and 10%, Manufactured by Precorp Co., Spanish Fork, UT); BAM coated WC; and (AlCrSi/Ti)N coated WC tool(by Fraunhofer USA, MI). The BAM coating was 3.5 μm thick deposited on the uncoated WC by the sputtering method. The (AlCrSi/Ti)N coated tool was WC 7.3 μm thick deposited on the uncoated WC by the cathodic arc deposition technology. The spindle speed was 6000 RPM, and the feed was 0.0762mm/rev in CFRP. A water-soluble coolant (Kool Mist. Formula #78) was used as spray mist during the experiment. Each drill bits was used to drill 140 holes.

The tool profile has been measured using a VHX-6000 confocal laser microscope (Itasca, Illinois, USA), which has been reported in previous publications [4,20]. Surface Roughness Parameters

were measured using has been measured using Roughness Measuring Profilometer (Mituyoto, Kanagawa, Japan) according to ISO 1997 roughness standard. The evaluation length was 6 mm to obtain as much as roughness possible along with the hole thickness. Surface roughness has been measured across the half holes in three consecutive holes every 40-hole interval, at holes 1-3, 39-41, 79-81, 119-121 of the CFRP hole, as shown in the schematic in Figure 2. The SEM images of the machined surfaces have been taken using Quanta 3D 200i (Thermo Fisher Scientific, Waltham, MA, USA).



Figure 1 The experimental set up [4]

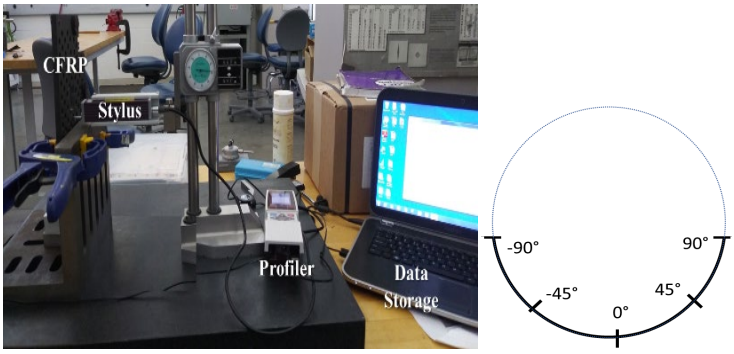


Figure 2 Measuring of surface roughness in half hole (left), location of the measurement (right)

3. RESULTS

3.1 Categorization of Tool Edge Geometry

This section aims to categorize the cutting edge of the tool. Continuous drilling with a tool causes changes in cutting-edge geometry. The tool edge geometry has been categorized into sharp, honed, and honed and chamfered in the machining of metal and metal matrix composite[13–17]. A schematics of tool edge geometry is shown in Figure 3. This approach is applied in this section to categorize the cutting-edge geometry as the cutting edges obtained from the tool profile show a similar geometric feature, as discussed in the literature. The cutting edge geometries obtained at hole 1, hole 40, hole 80 and hole 120 of this experiment are shown in Figure 4 according to categories described.



Figure 3 The microgeometry of cutting tool reported by Zhao et al. (2017) [21]

Initially, the sharp tools are sharp and become honed because of tool wear, which becomes chamfered due to further tool wear. In the beginning, the sharp edge receives the forces concentrated at a point, and the endure higher stress leading to higher materials removal. Hence, the sharp tool edge becomes honed, which eventually becomes chamfered and honed because of further tool wear. The edge strength of the tool edge varies depending on the edge geometry. Experimentally, the sharp edge creates a finer surface, while the honed edge creates rougher surfaces in metal machining [13–17]. Comparing Figure 3 and Figure 4, the existence of honed edge, chamfered edges and chamfered and honed edges are proven in CFRP machining.

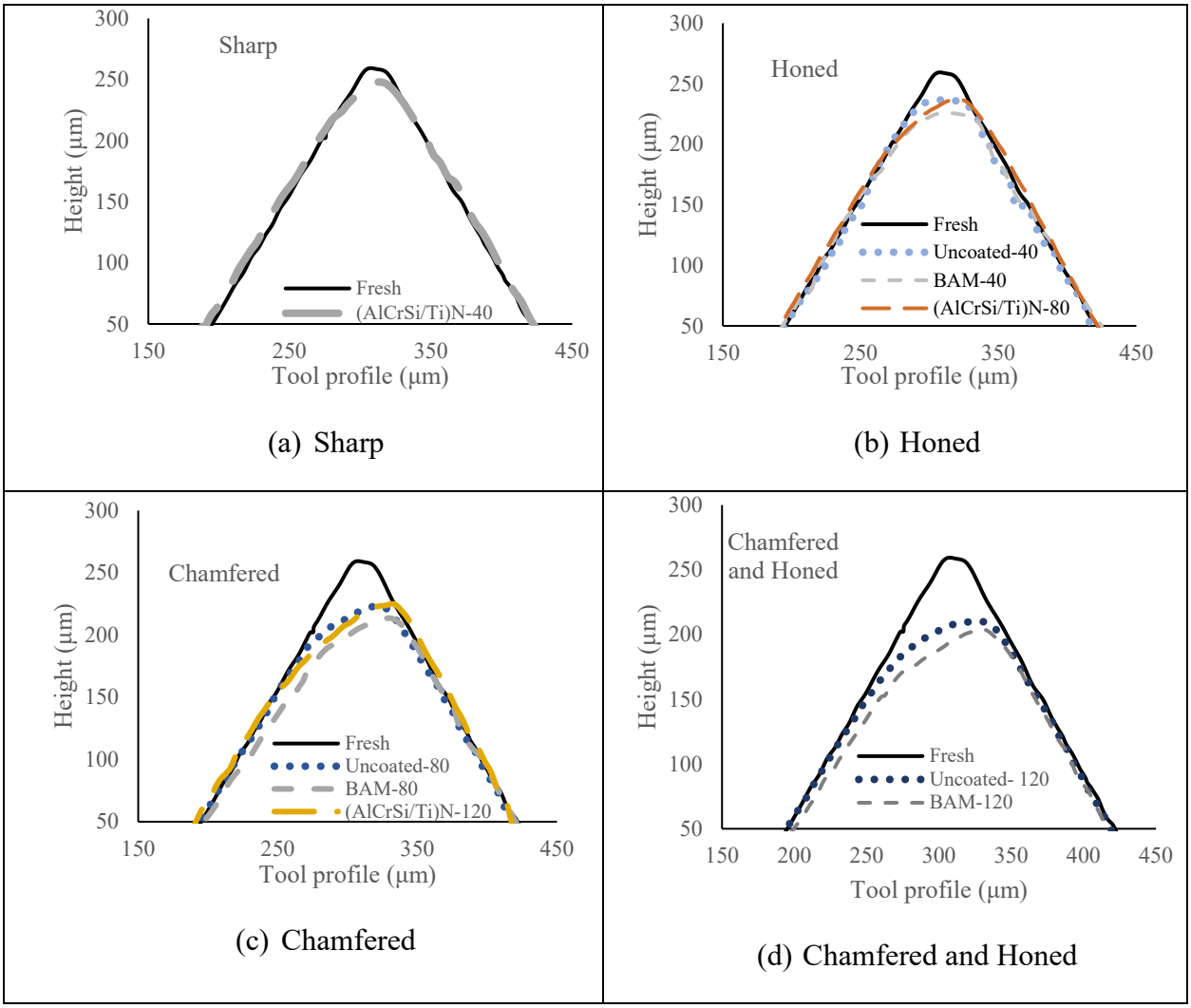


Figure 4 The Tool Edge Geometry according to the categorization for the uncoated, BAM coated and (AlCrSi/Ti)N coated tool from hole 1 to hole 120

Table 1 represents the flank wear area of the three drills obtained from the previous experiment along with the tool geometry type mentioned above [43]. All the tools had sharp edges before drilling any hole. The uncoated tool edge transformed into honed shape at hole-40 because of edge rounding and flank wear of 48 μm and started to become chamfered and honed followingly with further flank wear. The values of flank wear of uncoated tool at hole 80 and hole 120 are respectively 106 μm and 135 μm. Observing the tool contour of BAM coated tools in Figure 4, the BAM coated tool showed both the honed and the chamfered and honed edges at different stages of this experiment. The sharp BAM coated tool became honed due at hole 40 because of excess tool wear in BAM coated tool. From Table 1, it is seen that the BAM coated tool experienced 99 μm flank wear, which is large in both flank wear and wear area than the uncoated tool at hole 40. However, after hole-40, the BAM coated tool became more chamfered and honed due to larger flank wear of more than 200 μm, while the uncoated tool has flank wear of fewer than 140 μm. Therefore, larger chamfering in BAM coated tool is noticed compared to the uncoated tool at hole 80 and hole 120. As seen in Figure 4 (b); both the uncoated and the BAM coated tool edge are honed at hole 40, the (AlCrSi/Ti)N-coated tool at hole 80. The (AlCrSi/Ti)N-coated tool pertained to the sharp edge until hole 40 because of the least material removal due to better adhesion to the tool substrate. It is noted that the (AlCrSi/Ti)N coated tool at hole 40 is characterized by the least amount of wear area of 636 μm^2 according to Table 1. The better adhesion results from the existence of alternating layers of nano-coating and comparable substrate coating stiffness of the (AlCrSi/Ti)N coated tool resulted in the least amount of flank wear. Because of the aforementioned reasons, the (AlCrSi/Ti)N coated tool edge experienced honing and chamfering much slower compared to the BAM coated and the uncoated tool. That is why, this tool was still sharp until hole 40, as seen in Figure 4 (a); and became honed at hole 80 as seen in Figure 4 (b); the honed edge was induced by chamfering at hole 120 ensured by the tool profile in Figure 4 (c).

On the other hand, the cutting edge of other tools (BAM and Uncoated) became honed and chamfered much earlier compared to the (AlCrSi/Ti)N coated tool. Finally, the sharp tool edges are obtained for hole 1 for all drill and at hole 40 for (AlCrSi/Ti)N coated drill, shown in Figure 4 (a). After honing, the tool enters into chamfering, the third stage of geometry transformation. The honed cutting edges are obtained for uncoated hole 40, BAM hole 40 and (AlCrSi/Ti)N hole 80 in Figure 4 (b). Then chamfered cutting edges are identified at uncoated hole 80, BAM hole 80 and (AlCrSi/Ti)N 120, in Figure 4 (c). The chamfering occurs due to further material removal from the tool. Following to chamfering of the tool, further tool wear causes the tool to enter the fourth geometric transformation, when the tool becomes chamfered and honed, as seen in Figure 3. The uncoated tool and BAM coated tool edges at hole-120 are chamfered and honed. Meanwhile, the (AlCrSi/Ti)N coated tool even did not become hone and chamfered until hole 120. The tool geometries are clustered according to the categories stated in Table 1.

Table 1 The categorization of the cutting edge geometry at different holes of the experiment for the uncoated, BAM coated and (AlCrSi/Ti)N coated tool along with tool wear area

	Uncoated			BAM			(AlCrSi/Ti)N		
Hole	Edge Geometry	Flank wear (μm)	Wear Area (μm^2)	Edge Geometry	Flank wear (μm)	Wear Area (μm^2)	Edge Geometry	Flank wear (μm)	Wear Area (μm^2)
1	Sharp	-	-	Sharp	-	-	Sharp	-	-
40	Honed	48	1822	honed	99	2417	Sharp	47	636
80	Chamfered	106	2955	Chamfered	235	4453	Honed	73	1346
120	Hone and Chamfered	135	3804	Hone and Chamfered	281	5560	Chamfered	121	2426

3.2 Tool Edge Geometry and Surface Roughness

The surface roughness is believed to be related to cutting tool geometry. The surface roughness of the holes 1-3, 39-41, 79-81, and 119-121 drilled by each tool have been measured. Likewise, the roughness holes corresponding to the specific tool geometries have been analyzed in this section. Table 2 represents the changes of average surface roughness (Ra) and mean surface roughness (Rq) of the tool edge categories; 'sharp', 'honed', 'chamfered' and 'chamfered and honed'. The Average Ra and Average Rq in this table is the average of all the Ra and Rq values obtained from half-holes (five measurements in each hole) for all corresponding hole drilled. According to Table 2, the sharp tool edges create at average Ra of 2.48 μm, and the average Rq of 4.52 μm. As the tool becomes honed, the average Ra and average Rq increases to 2.68 μm and 4.70 μm. And, the chamfered tool edges generate machined surface of 3.08 μm (average Ra) and 5.44 μm (average Rq). It is noticeable that the roughness of the machined surfaces increases again as the tool edge becomes chamfered from honed. A similar phenomenon has been reported in metal machining when the roughness increased as the tool become chamfered from honed. The edge strength increases as the tool become chamfered from hone [13–17] and create a rougher surface. In addition to that as the tool becomes more chamfered, the increased tool edge radius causes further pushes to the fibers instead of cutting. This interplay causes roughness to increase. According to Table 2, the chamfered and honed edges generates surfaces of roughness values of 2.85 μm (average Ra) and 5.07 μm (average Rq). Both the average roughness value and mean roughness value decreased from their respective values (Average Ra= 3.08 μm, Average Rq=5.44 μm). Such decrease in the roughness may have been caused due to matrix smearing in CFRP machined surface due to softening of the matrix due to increased heat generation [9,24]

Table 2 The Average Surface Roughness (Ra) and Mean Surface Roughness (Rq) with the standard deviation for different types of cutting edge geometry

Tool Edge Geometry type	Average Ra (µm)	Average Rq (µm)
Sharp	2.48 ± 1.64	4.52 ± 3.55
Honed	2.68 ± 1.38	4.70 ± 2.67
Chamfered	3.08 ± 1.43	5.44 ± 2.67
Chamfered and Honed	2.85 ± 1.24	5.07 ± 2.66

Total height (Rt) and 10-point height (Rz) are also important parameters in CFRP machining. The bar chart in Figure 5 shows the change of average total height (Average Rt value) and average 10-point height (Average Rz value) for all types of tool edge geometry. The Rt value is 46.38 µm for sharp cutting edges, while the value is 58.38 µm and 63.13 µm respectively for honed edge and chamfered edge. This resembles that the Rt value larger for the honed edge than the sharp edge, and larger for the chamfered edge than the honed edge. The Rt value increases due to deeper and frequent fibers pulled out. However, the Rt value decreased down to 55.16 µm from 63.13 µm. Such a decrease can be attributed to the matrix smearing, as the smeared matrix fills the gap caused by fiber pullouts and other occasional found in CFRP machining. With respect to the tool edge geometry, the 10-point height (Rz) follows a similar trend like Rt of Rt as seen in Figure 5 due to the stated reasons above.

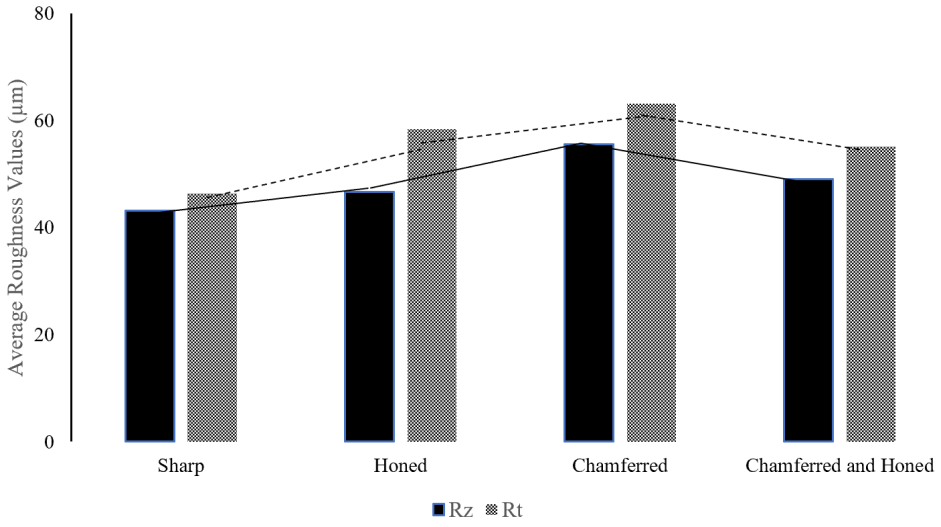


Figure 5 The Average Surface Roughness (Ra) and Mean Surface Roughness (Rq) with the standard deviation for different types of cutting edge geometry (The Average Ra and Average Rq in this table is the average of all the Ra and Rq values obtained from half-holes (five measurements in each hole) for all corresponding hole drilled)

Table 3 presents the average peak height (Rp) and average valley depth (Rv) measured for different edge geometry. The peak height, Rp, physically refers to the potential furthest position of the uncut fibers in CFRP, and the valley depth (Rv), refers to the deepest fiber pull-outs on CFRP machined surface[25,26]. For sharp tools, the average Rp value is 12.13 µm, while the Rp value is

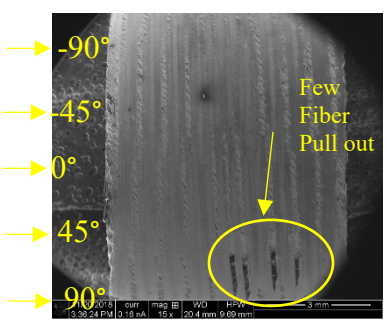
15.57 µm and 18.78 µm respectively for honed edges, and chamfered edges. Such increment refers to the larger uncut fiber, which is true as the dull tool leaves more uncut fibers in CFRP. The Rp values again drop down for the chamfered and honed tools to 16.67 µm from 18.78 µm in chamfered edges. This again hints to sever matrix smearing that reduces the roughness. Additionally, the average Rv value increased steadily from sharp edge to honed edge and chamfered edge; again decreased down when the honing induced the chamfering.

Table 3 The average peak height (Rp) and Average valley depth (Rv) in the experiment

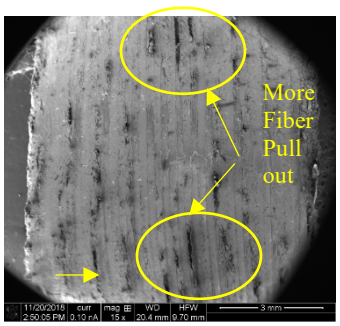
Tool Edge Geometry type	Average Rp (µm)	Average Rv (µm)
Sharp	12.13 ± 12.84	31.09 ± 29.65
Honed	15.57 ± 12.71	31.16 ± 20.32
Chamfered	18.78 ± 12.20	36.82 ± 21.08
Chamfered and Honed	16.74 ± 13.55	32.33 ± 17.83

3.3 Tool Edge Geometry and Surface Morphology from SEM Images Observation

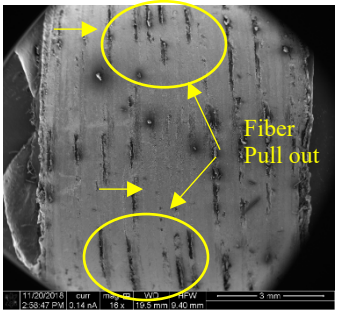
The SEM images of the machined surface have been taken to observe the surface characteristics. Figure 6 represents the SEM images of the machined surface for every cutting edge. According to Figure 6 (a), the sharp cutting edge machined surface looks smoother with few locations of fiber pullout in a few plies in 90° direction, which is intrinsic in CFRP machining. Usually, in drilling of CFRP fiber pull out happens when the relative angle between fibers and the cutting tool is around 135° due to bending causing fiber fracture happening in the beneath the surface [6,27]. For machined surface obtained by honed edge [in Figure 6 (b)] and for chamfered edges [in Figure 6 (c)], the presence of fiber pullout is more frequent and fiber pull out depth looks deeper. These SEM images are the evident cause of the increased roughness for honed edge and the chamfered edge of the CFRP surface discussed in the previous section. However, Figure 6 (d) is the SEM image of the machined surface of the honed and chamfered edge. It is evident that the matrix is smeared on the CFRP surface, and deep pockets are less visible, especially in the direction of 90° and -90°. These pieces of evidence of matrix smearing portray the underlying reason for roughness decrease in the previous section.



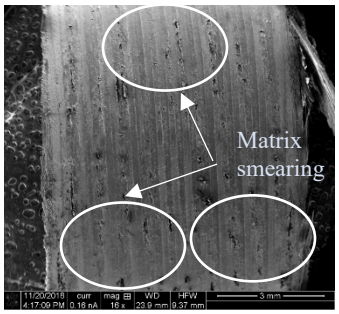
(a) Sharp



(b) Honed



(c) Chamfered



(d) Honed and Chamfered

Figure 6 SEM images of the drilled holes using (a) Sharp cutting edge, (b) honed cutting edge[Presence of Fiber Pull out in Yellow ellipse], (c) chamfered cutting edge [Presence of Fiber Pull out in Yellow ellipse and (d) honed and chamfered cutting edge [Presence of matrix smearing in white ellipse]

4. CONCLUSIONS

This paper presented a primary investigation to study the relation of cutting edge geometry in CFRP drilling with the uncoated WC tool, BAM Coated and (AlCrSi/Ti)N coated tool. The followings are the conclusions inferred from the experimental findings.

1. Like the metal and metal matrix composite machining, honed, chamfered, chamfered and honed cutting edges are observed in CFRP machining. The sharp tool edge first turned into a honed edge due to tool wear. And, the additional flank wear creates chamfer on the honed edges. The coating, especially the (AlCrSi/Ti)N, delayed the changes in cutting edge geometry. The (AlCrSi/Ti) coated drill remained almost sharp until hole 40, while the edge geometry changed into honed shape at hole 80 followed by chamfering at hole 120. On the other hand, the uncoated tool and the BAM coated tool, severely susceptible to tool wear, became honed at hole 40. Meanwhile, the uncoated tool became chamfered at hole 80 and BAM coated tool edge was chamfered and honed at hole 80. In the end, at 120, all the tools had chamfered and honed cutting edge except the (AlCrSi/Ti)N coated tool, which remained chamfered.
2. The roughness of the machined surface has a strong relation to cutting edge geometry. The surface roughness increase if the tool edge is transformed from sharp to honed, and increased further if the cutting edge is chamfered. The chamfered edge creates the largest roughness (Ra, Rq, Rt, Rz, Rp, Rv) on the machined CFRP surface. However, when the tool edge is ‘chamfered and honed’, the roughness decreases. with the onset of matrix smearing.
3. Further extensive study is required to understand the surface roughness and tool geometry relationship.

5. REFERENCES

[1] Holmes M. Global carbon fibre market remains on upward trend. Reinforced Plastics 2014;58:38–45. https://doi.org/10.1016/S0034-3617(14)70251-6.

[2] Hale J. Boeing 787 from the Ground Up. Aero 2006;4:17–23. https://www.boeing.com/commercial/aeromagazine/articles/qtr_4_06/article_04_1.html

[3] Schade DW. Analysis of the light weight fiber reinforced plastics value chain with regard to the German industry in its global context n.d.:54. https://www.m-five.de/pdf/M_Five_Light_Weight_Composites_Value_Chain_in_GER_FINAL_2017.pdf
[4] Swan S, Bin Abdullah MS, Kim D, Nguyen D, Kwon P. Tool Wear of Advanced Coated Tools in Drilling of CFRP. Journal of Manufacturing Science and Engineering 2018;140:111018-111018–10. https://doi.org/10.1115/1.4040916.
[5] Nguyen D, Voznyuk V, Bin Abdullah MS, Kim D, Kwon PY. Tool Wear of Superhard Ceramic Coated Tools in Drilling of CFRP/Ti Stacks. MSEC2019, Volume 2: Processes; Materials: 2019. https://doi.org/10.1115/MSEC2019-2843.
[6] Hou G, Qiu J, Zhang K, Cao S, Cheng H, Luo B, et al. Comparative tool wear and hole quality investigation in drilling of aerospace grade T800 CFRP using different external cooling lubricants. The International Journal of Advanced Manufacturing Technology 2020;106:937–51. https://doi.org/10.1007/s00170-019-04554-9.
[7] Ahsan MA, Hosur M, Tareq SH, Hasan SMK. Quasi-static compression characterization of binary nanoclay/graphene reinforced carbon/epoxy composites subjected to seawater conditioning. Materials Research Express 2020;7:015033. https://doi.org/10.1088/2053-1591/ab62fb.
[8] Soutis C. Fibre reinforced composites in aircraft construction. Progress in Aerospace Sciences 2005;41:143–51. https://doi.org/10.1016/j.paerosci.2005.02.004.
[9] Kim D, Beal A, Kwon P. Effect of Tool Wear on Hole Quality in Drilling of Carbon Fiber Reinforced Plastic–Titanium Alloy Stacks Using Tungsten Carbide and Polycrystalline Diamond Tools. Journal of Manufacturing Science and Engineering 2015;138:031006. https://doi.org/10.1115/1.4031052.
[10] Wang F, Qian B, Jia Z, Fu R, Cheng D. Secondary cutting edge wear of one-shot drill bit in drilling CFRP and its impact on hole quality. Composite Structures 2017;178:341–52. https://doi.org/10.1016/j.compstruct.2017.04.024.
[11] Montoya M, Calamaz M, Gehin D, Girot F. Evaluation of the performance of coated and uncoated carbide tools in drilling thick CFRP/aluminium alloy stacks. The International Journal of Advanced Manufacturing Technology 2013;68:2111–20. https://doi.org/10.1007/s00170-013-4817-0.
[12] Liu D, Tang Y, Cong WL. A review of mechanical drilling for composite laminates. Composite Structures 2012;94:1265–79. https://doi.org/10.1016/j.compstruct.2011.11.024.
[13] Rahim EA, Mohid Z, Hamzah MR, Yusuf AF, Rahman NA. Performance of Tools Design when Helical Milling on Carbon Fiber Reinforced Plastics (CFRP) Aluminum (Al) Stack. Applied Mechanics and Materials 2013;465–466:1075–9. https://doi.org/10.4028/www.scientific.net/AMM.465-466.1075.
[14] Sandvik Coromant. User's Guide- Machining carbon fbre materials n.d. https://www.sandvik.coromant.com/sitecollectiondocuments/downloads/global/technical%20guides/en-gb/c-2920-30.pdf
[15] Denkena B, Lucas A, Bassett E. Effects of the cutting edge microgeometry on tool wear and its thermo-mechanical load. CIRP Annals 2011;60:73–6. https://doi.org/10.1016/j.cirp.2011.03.098.
[16] Denkena B, Biermann D. Cutting edge geometries. CIRP Annals 2014;63:631–53. https://doi.org/10.1016/j.cirp.2014.05.009.

[17] Zhang L, Ren C, Ji C, Wang Z, Chen G. Effect of fiber orientations on surface grinding process of unidirectional C/SiC composites. Applied Surface Science 2016;366:424–31. https://doi.org/10.1016/j.apsusc.2016.01.142.
[18] Zhao T, Agmell M, Persson J, Bushlya V, Ståhl JE, Zhou JM. Correlation between edge radius of the cBN cutting tool and surface quality in hard turning. Journal of Superhard Materials 2017;39:251–8. https://doi.org/10.3103/S1063457617040050.
[19] Zhao B, Ding WF, Dai JB, Xi XX, Xu JH. A comparison between conventional speed grinding and super-high speed grinding of (TiCp + TiBw) / Ti–6Al–4V composites using vitrified CBN wheel. The International Journal of Advanced Manufacturing Technology 2014;72:69–75. https://doi.org/10.1007/s00170-014-5656-3.
[20] Abdullah MSB. EFFECTS OF FIBER ORIENTATIONS AND PROPERTIES ON TOOL WEAR AND MACHINED SURFACE QUALITY IN MACHINING OF CARBON FIBER REINFORCED PLASTICS LAMINATE. Washington State University, 2019. https://www.researchgate.net/publication/338701977_EFFECTS_OF_FIBER_ORIENTATIONS_AND_PROPERTIES_ON_TOOL_WEAR_AND_MACHINED_SURFACE_QUALITY_IN_MACHINING_OF_CARBON_FIBER_REINFORCED_PLASTICS_LAMINATE
[21] Zhao T, Zhou JM, Bushlya V, Ståhl JE. Effect of cutting edge radius on surface roughness and tool wear in hard turning of AISI 52100 steel. The International Journal of Advanced Manufacturing Technology 2017;91:3611–8. https://doi.org/10.1007/s00170-017-0065-z.
[22] ﷿zel T, Hsu T-K, Zeren E. Effects of cutting edge geometry, workpiece hardness, feed rate and cutting speed on surface roughness and forces in finish turning of hardened AISI H13 steel. The International Journal of Advanced Manufacturing Technology 2005;25:262–9. https://doi.org/10.1007/s00170-003-1878-5.
[23] Raj DS, Karunamoorthy L. Study of the Effect of Tool Wear on Hole Quality in Drilling CFRP to Select a Suitable Drill for Multi-Criteria Hole Quality. Materials and Manufacturing Processes 2016;31:587–92. https://doi.org/10.1080/10426914.2015.1004713.
[24] Ramulu M, Wern CW, Garbini JL. Effect of fibre direction on surface roughness measurements of machined graphite/epoxy composite. Composites Manufacturing 1993;4:39–51. https://doi.org/10.1016/0956-7143(93)90015-Z.
[25] Landon Y, Cherif M. Characterization of the Surface Quality of Holes Drilled in CFRP Laminates. AMR 2013;698:107–16. https://doi.org/10.4028/www.scientific.net/AMR.698.107.
[26] Rimpault X, Chatelain J-F, Klemberg-Sapieha JE, Balazinski M. Surface profile texture characterization of trimmed laminated composite in the stacking sequence direction. Measurement 2016;91:84–92. https://doi.org/10.1016/j.measurement.2016.05.039.
[27] Ramulu M, Kim D, Choi G. Frequency analysis and characterization in orthogonal cutting of glass fiber reinforced composites. Composites Part A: Applied Science and Manufacturing 2003;34:949–62. https://doi.org/10.1016/S1359-835X(03)00203-3.